DOI: 10.14529/jsfi260103

Ionic and Water-Saturated Clusters in Self-Healing Polydimethylsiloxanes Modelled by Molecular Dynamics

Tatiana M. Makarova[1], *Ekaterina V. Bartashevich*[1]

Elaboration of new self-healing polymer materials with improved properties such as room-temperature healing and sufficient mechanical performance is a complicated task. In our study, we present the groundwork for construction of multicomponent systems for polydimethylsiloxane-based polymers via condensation in molecular dynamics resembling the simulated annealing protocol. Upon the self-organization according to the force field that model the intermolecular interactions, all the compounds of the "siloxane equilibration" system reproducibly assembles in a polydisperse structure with ionic and water-saturated aggregates. Around these aggregates, the negatively charged polymer terminal groups are oriented, along with ions of initiators and residual water. At the temperature of self-healing, the outer layers of the aggregates intensively exchange with each other. Thus, the molecular dynamic simulations shed light on crucial structural and dynamical properties on a molecular level that can influence the self-healing process, which would be useful in further targeted development of these materials having a prospect in cable products.

Keywords: self-healing materials, PDMS, "siloxane equilibration", MD simulation.

Introduction

Nowadays the requirement for high-tech polymer-contained devices in various areas permanently increases, entailing the problems of labored reparation of them in case of mechanical or electrical damage. This problem particularly manifests in electronic devices, when a breakdown can distort the mechanical integrity of a dielectric material disabling thus a rather expensive device. To overcome this problem, polymers with self-healing properties, i.e., able to heal the occurring mechanical defects in it, have attracted significant interest as promising participants of a sustainable development concept [3, 27]. Self-healing materials are comprised by various types of polymers possessing exchangeable bonds or interactions with relatively low activation energy threshold, which are able to reversibly cleavage and reform, providing mobility of the chains and regaining mechanical strength and integrity after the damage. These exchangeable bonds may be noncovalent (hydrogen bonds [9, 52, 57], ionic interactions [12, 29, 37] etc.) or covalent [46, 55] (for example, Diels—Alder reversible condensation [6, 17], donor-acceptor metal coordination [15, 28, 34, 51], imine bond [47, 60], disulfide bond [35, 42], dynamic urea bond [56], boron ester bond [7, 10, 58], oxime ester [20] and many others), or the polymer can contain a combination of both types.

Polysiloxane-based self-healing materials are comprised by chains of the Si–O– sequence with the feature of recombination of Si–O bonds between two different chains. High flexibility and low rotation energy barrier of the polysiloxane chains [32], provide excellent mobility of the chains and thus high efficacy of self-healing, however, along with low mechanical performance. Nevertheless, in case of electronic devices including those in biomedicine, the effectiveness, rate and autonomy of self-healing is a priority. Also, such peculiarities of self-healing polysiloxanes as optical transparency, flexibility, high environmental and thermal stability provide their wide potential application in electronics and wearable devices [19, 26, 53], soft robotics [58], microfluidics [39] and special indispensability for biomedical devices due to their complete biocompatibility [33, 50, 54]. Extremely low (about -120°C) glass transition temperature, T_g, of polysiloxanes

[1]South Ural State University, Chelyabinsk, Russian Federation

makes them a very attractive object for modifications in order to approach the room temperature effective self-healing via, for example, adding of a silicone exchange catalyst [8, 24] or additional type of reversible bonds with lower activation energy [14, 25, 40]. However, these methods may significantly increase the material cost and, what is more important, decrease one of the most valuable unique polysiloxane properties such as biocompatibility. Therefore, development of the room temperature silicone self-healing materials with minimal chemical interventions is a challenging task. To find the pathway of such modification, a detailed picture of the self-healing mechanism at the molecular level would be indispensable.

In all the available literature, the self-healing of polyorganosiloxanes is attributed to the "siloxane equilibration" reaction, in which an electronegative terminus of one chain attacks a middle of another chain by S_N2 mechanism, upon which the second chain is shortened, and the first one is lengthened. The S_N2 mechanism of this reaction is confirmed both by quantum chemical calculations using DFT methods [13] and experimental methods [36, 44]. Indeed, it is the presence of charged $–Si(CH_3)_2O^-$ terminal groups that imparts self-healing properties to siloxane materials, while neutralization of the charged chain ends deprives the materials of this ability [59]. However, detailed atomic and molecular structure of the multicomponent polymeric system could provide crucial information for understanding the self-healing process and its relation with desired mechanical performance.

In our study, for computational investigations, the "siloxane equilibration" compounds, previously obtained as follows [38, 41], were selected as the most simple compounds of their class. These polymers were synthesized by anionic polymerization of the D_4 reagent (octamethyltetracyclosiloxane) with a small amount of its dimer, *bis*-D_4 reagent, every molecule of which contains C–C bond and, being included into the polymer, provides ethylene crosslinks between two linear PDMS chains. The polymerization is initiated by an anion, typically OH^-, and the most common initiators are $N(CH_3)_4OH$ (TMAOH) [59] or KOH. It was found that the quality and type of the initiator can influence the self-healing temperature and other material properties. This and other features can hardly be explained without understanding of the PDMS-based "siloxane equilibration" material organization at the molecular level. The reliable structural and dynamical modeling could reveal some crutial heterogeneity in its structure and its role in the self-healing processes.

Therefore, molecular dynamics (MD) simulations were performed for investigation of this issue. Though this method does not imply rearrangements of covalent bonds, it is indispensable to model the polymer organisation at the molecular level and assess the possibility of a certain reaction according to the distance between the reaction centers. Task-oriented material design with purpose properties, attempted to reach certain values by variation of chemical composition and structure, is more efficient when it is based on a structure-property relationship model. The MD simulation method has approved itself to be appropriate and conclusive for investigation of irregular structure of polymer materials, including those with self-healing abilities [23]. In this research, we exploited it to obtain the three-dimensional dynamic picture of the "siloxane equilibration" materials and to establish the processes guiding its self-healing.

Virtual simulation provides insights into systems with different parameters easily fine-tuning in the model compared to the synthesis, such as the initiator effectiveness or a small water impurity in the investigated polymer. To address this issue, we designed several theoretical systems along with experimentally based varying parameters such as the counterion type, the initiator effectiveness or an average chain length.

To establish the detailed structure of the self-healing PDMS materials, a simulation protocol that would chemically-friendly guide the system self-organization is required. If any initial guess for the irregular multicomponent polymer structure is absent, it is possible to start from the cell with randomly distributed components in it, which is anyway far from the real structure and thus requires the surmounting of a lot of substantial energy barriers on the way to the potential minimum with the most reliable structure of the material organization. The simulated annealing protocol [43] provides such kind of a global optimization strategy which at the beginning point supplies the system with an energy sufficient to overcome barriers on its energetic landscape and then gradually reduces the additional energy which steers the system towards the global energy minimum. In our study, we adopted a similar strategy to the MD simulation of PDMS-based "siloxane equilibration" systems containing ions of different initiators, $N(CH_3)_4OH$ or KOH, in various concentration, and water molecules. The results of the proposed modelling protocol and the influence of the concentration of different ions were thoroughly analyzed.

The present article is organized into three main sections. The "Methods" section is devoted to computational protocol details, the "Results and discussion" section contains general description of MD simulation data and their interpretation. Conclusion points out the significance of the obtained results for understanding of the self-healing mechanism and potential directions of material development for its improvement.

1. Methods

1.1. System Design and Construction of the Polymer MM Models

We assumed that upon polymerization, each initiator anion creates one unbranched PDMS chain, while each *bis*-D_4 crosslink consumes two initiator anions for every opening ring, creating one cross-linked polymer molecule. Therefore, the average chain length in the system is defined by the ratios between the initial components (D_4, *bis*-D_4 and the initiator, KOH or $(CH_3)_4NOH$) and one more value – the initiator efficiency, i.e., the percentage of the initiator ions that participated in the nucleophilic substitution reaction and created an "opened" $-(CH_3)_2Si-OH$ group. Modeling of the systems with M_w according to the NMR and GPC data (58 kDa and 66 kDa) implied certain KOH efficacy and thus the presence of a certain number of unreacted OH^- in the system along with the initiator counterions. The corresponding amount of these ions were added to the systems (Tab. 1). Also, systems with different initiator efficiencies and calculated from it average chain lengths were similarly constructed.

The minimal number of chains was selected in order to provide the unfolded conformation of them in the simulation. For systems with large M_w amount above 40 chains was sufficient for this, while in the systems with a higher initiator efficiency we had opportunity to simulate a larger number chains. The lengths of individual chains were generated according to the Poisson distribution with a given mean, and these chains were arranged within a cubic cell at equal distances from each other in each of the three dimensions. Crosslinks were introduced into some of the chains according to the mass fraction of *bis*-D_4. The chain and the location within it for each crosslink were also chosen randomly, with the only assumption being that the crosslinks or chain ends must be separated from each other by at least six DMS residues.

Though PDMS is a highly hydrophobic material, it was supposed to absorb some amount of water. Thus, certain excess of water in the amount of 0.5% mass. was included into the models as a preliminary upper bound of water content.

Systems with $(CH_3)_4NOH$ were constructed in a similar manner, but K^+ ions were replaced with $(CH_3)_4N^+$ ions using an authoring Python script with the *cmd* library, and are denoted hereafter as PDMS-TMA systems (in names like PDMS-TMAOH-13 the last number means initiator effectiveness, here 13%). Otherwise, systems with KOH as an initiator are denoted as PDMS-KOH.

The full list of the constructed systems is the following:

- PDMS-K-100 with the initiator effectiveness of 100%;
- PDMS-K-30 with the initiator effectiveness of 30%;
- PDMS-K-13 (13.2% effectiveness, corresponding to the experimental M_w of 58 kDa);
- PDMS-K-10 (10.4% effectiveness, corresponding to the experimental M_w of 66 kDa);
- PDMS-TMA-13.

For them, the quantitative compound and other details are given in the Tab. 1. In it, M_n is given in a number of DMS residues, while nOH^- denotes the number of free unreacted anions in the system. After a number of chains and "=" its quantitative distribution along every dimension is given.

Table 1. The quantitative (in a number of molecules) composition of the "siloxane equilibration" material simulation cells

System name	Polymer chains	Cell, nm	M_n	Crosslinks	nOH^-	Cations	Water
PDMS-KOH-100	$216 = 2 \times 6 \times 18$	39	53	12	0	228	222
PDMS-KOH-30	$64 = 1 \times 2 \times 32$	58	197	12	177	253	248
PDMS-KOH-13	$64 = 1 \times 4 \times 16$	46	782	47	732	843	986
PDMS-KOH-10	$48 = 1 \times 4 \times 12$	52	890	41	756	845	843
PDMS-TMAOH-13	$64 = 1 \times 4 \times 16$	46	782	47	732	843	986

The construction of the systems was performed using a Python script with the *cmd* module. For systems with low initiator effectiveness (10 and 13%) long chains were folded into "rolls" from an unfolded D_4 structure with Si–O–Si–O and O–Si–O–Si torsion angles $\tilde{1}76°$ – the minimal value that allowed the chains to be folded without steric interference (Fig. 1a). After this, the cell was filled with water, and the required amount of randomly distributed ions and water molecules were added using the *gmx solvate* and *gmx genion* instruments of GROMACS software, respectively.

The molecular mechanical models of the PDMS residues, both for the linear and branched fragments, were prepared using the General Amber force field [49]. Partial charges were evaluated according to the RESP model [1]. The lacking parameters of covalent bonds and angles for DMS and crosslink residues were calculated by DFT method with M06–2X functional and 6–$311^{++}G^{**}$ basis set [30] along with parameters from [16].

1.2. Molecular Dynamics Simulation Protocol

We began the simulation at high temperature (about 800–1000 K) which ensured an easy overcoming of all the conformational barriers, and then linearly decreased it down to the room temperature, providing thus the system movement towards the most energetically optimal structure guided by forces of intermolecular interactions from the forcefield.

The MD simulations were carried out using GROMACS 2019.4 software [22, 48]. The time step of integration for equations of motion was 2 fs. The system coordinates were written to the *xtc* trajectory file every 20 ps. The lengths of all bonds were controlled using the LINCS

algorithm [21]. The temperature was maintained by the velocity rescaling thermostat with additional stochastic correction [4] with 0.1 ps coupling time. The pressure in NPT simulations was controlled by Berendsen barostat [2] with the coupling time of 5 ps. Ewald particle mesh with the sixth order of interpolation and a 0.1 nm grid step was used to threat long-range electrostatic interactions [11].

Every MD simulation was preceded by a geometry optimisation by the Broyden—Fletcher—Goldfarb—Shanno algorithm [5]. The sequence of all calculation procedures upon the system modelling is given in Tab. 1.

1.2.1. Results and discussion

At the initial stage of the system modelling, initial unit cells with PDMS chains were constructed. We applied the software previously developed by us for modeling of lesser polymer cells [31] that was based on various probabilistic algorithms which essentially randomly distributed components in the cell, creating a system that reproduces the required ratios of initial reagents and the average chain length (with the individual chain lengths distributed according to the Poissons law). Thus constructed systems with PDMS chains, ions, residual water and D_4 reactant underwent a procedure of *in silico* condensation to achieve a deep equilibration during the system self-organization.

In this procedure, after potential energy optimization, MD simulation is to be carried out at constant volume and high temperature that is significantly higher than the physical polymer could sustain (up to 1073K, see Tab. 1). During this simulation, the polymer chains and other components intensively mix with each other, remaining distributed throughout the cell without significant condensation in a confined region.

At this step, for systems with long PDMS chain a crutial problem arose: the polymer chains began to "curl" folding on themselves (which would result into unnatural conformations upon further condensation) rather then interact with each other due to large interchain distances. Prevention of the curling by mere temperature increase entailed a high probability of triggering the LINCS algorithm, aborting the simulation. A solution was found in reducing the free space in the initial cell by folding the polymer chains into artificial helices as tightly as the PDMS structure allowed without a steric clash of the van der Waals radii of the atoms (Fig. 1a). The dense PDMS chains packed into such kind of "rolls" did not inflict tense system conformation in further simulations: the chains unrolled during the first tens of the NVT trajectory (Fig. 1c, left). Therefore, this chain twisting was used to construct the systems with long polymer chains.

At the next step of the simulation protocol, the system was slowly cooled to ambient or 100°C temperature. Upon this process, molecules and ions aggregated according to their interaction forces, thus adopting the most natural conformation and mutual arrangement (see Fig. 1c, right).

At the final stage, the systems at 25 or 100°C were extracted from the condensation trajectory after stabilization as starting systems for further simulations. After the geometry optimization, final trajectories of 500 ns length were obtained for each type of the system (all kinds of simulated systems are described in Methods). The final density that the modeled systems reached was about 0.95 (Fig. 1), which falls within the range of 0.91–1.00 for PDMS materials [45].

In all the simulated systems we observed an aggregation of positively charged counter-ions and the self-organization of charged and polar groups and molecules around these aggregates (Fig. 2). These aggregates assembled reproducibly in various cells with different compositions and in all the MD runs with different ratios of components (Tab. 1).

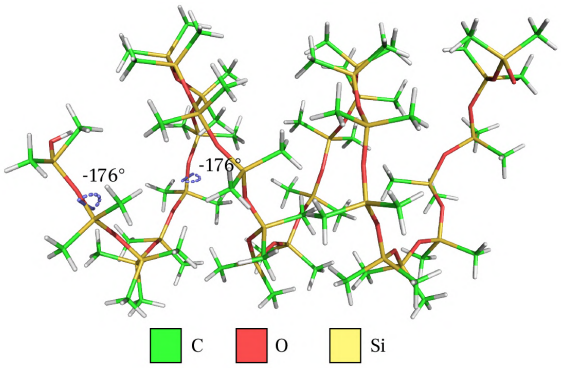

(a) Initial compacted conformation of PDMS chains

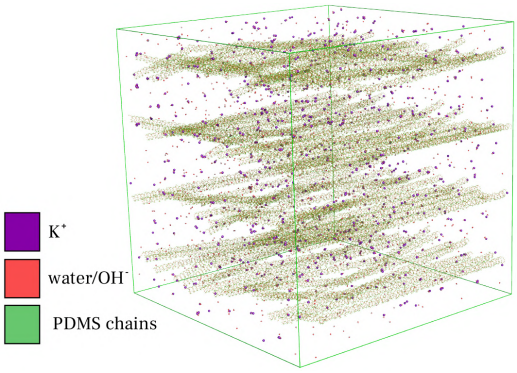

(b) General view of the starting system with "rolled" PDMS chains and ions

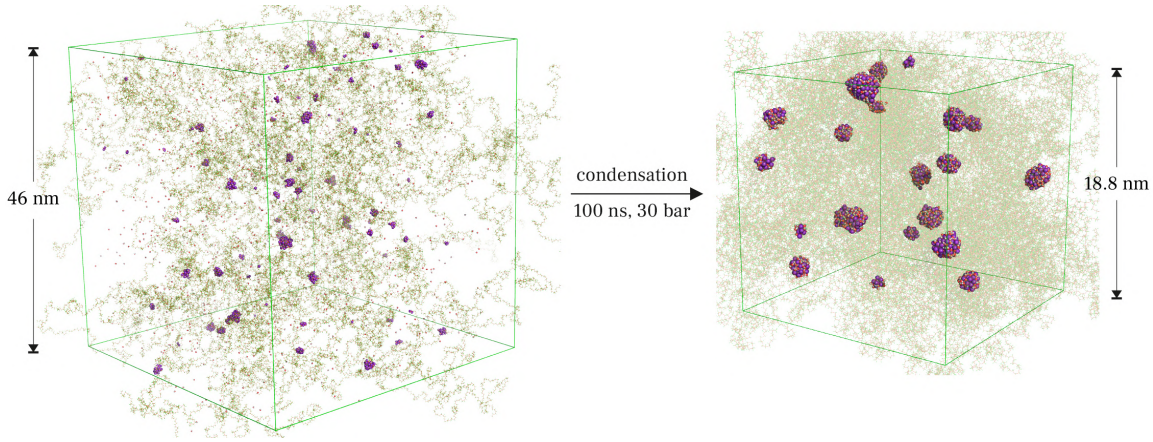

(c) Condensation of the polymer material cell after short NVT simulation

Figure 1. Construction and condensation of polymer material simulation cells

We observed that the size and distribution of the aggregates heavily depended on the initiator effectiveness. For a system with 100% effectiveness (without free OH^- in the polymer), the average ionic aggregate size was about 5–6 cations (Fig. 2a). As initiator efficiency decreased, the aggregate size increased due to residual OH^- anions incorporating between cations, thereby enhancing their retention (Fig. 2b). The greater was the fraction of unreacted initiator remnants, the larger was the average size of the aggregates, increasing up to more than 40 K^+ cations at 10–13% effectiveness (Tab. 1). With extremely low initiator effectiveness (10–13%), the number of K^+ and OH^- ions in the system was nearly equal, which provided formation of stable ionic aggregates of many tens of ions (Fig. 2c).

The aggregates in our systems had a more complex structure than any other ionic aggregates previously described [18]. All negatively charged termini of the polysiloxane chains were "anchored" by cationic aggregates. All water molecules, as well as polar hydrophilic groups at the beginning of the chains at the site of nucleophilic OH^- attachement, were also coordinated around the ionic aggregates, so that the space between the aggregates was filled only with low-polarity lipophilic PDMS chains. At larger aggregate sizes, they attracted even less polar residues, such as forming ethylene crosslinks in the chains (Fig. 2c, right). Thus, all the negatively charged groups that initiate the siloxane exchange reaction appeared to be trapped on the surface of the aggregates in our model. This should be taken into account for future investigation of the siloxane equilibration kinetics.

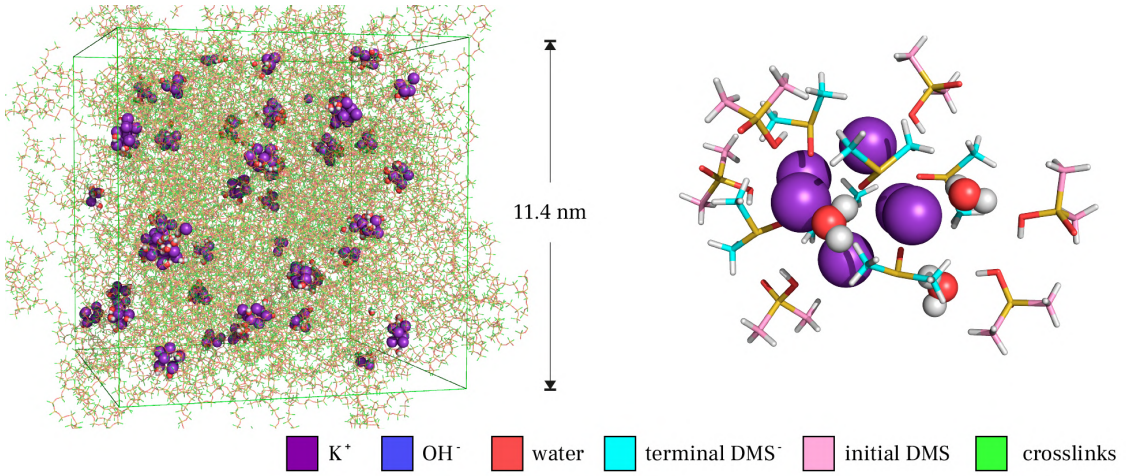

(a) Initiator effectiveness 100%, no OH^- ions in the system

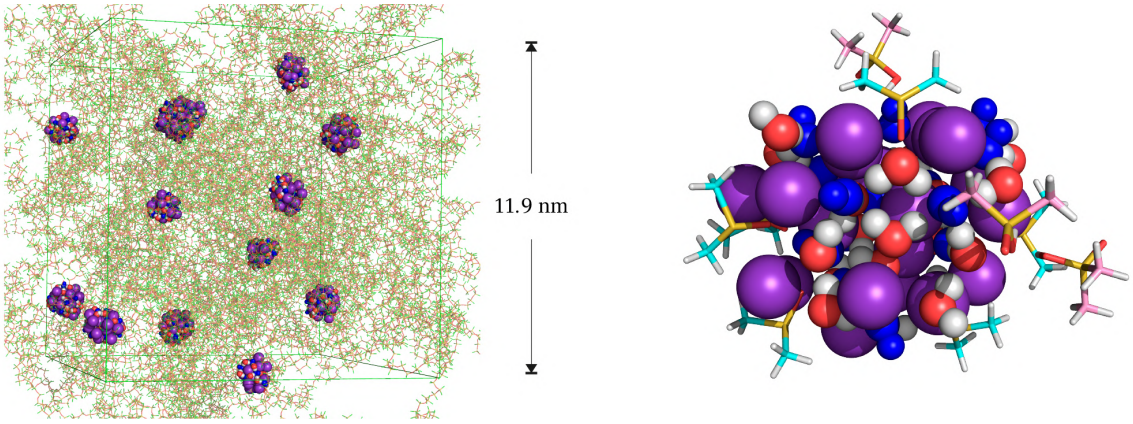

(b) Initiator effectiveness 30%

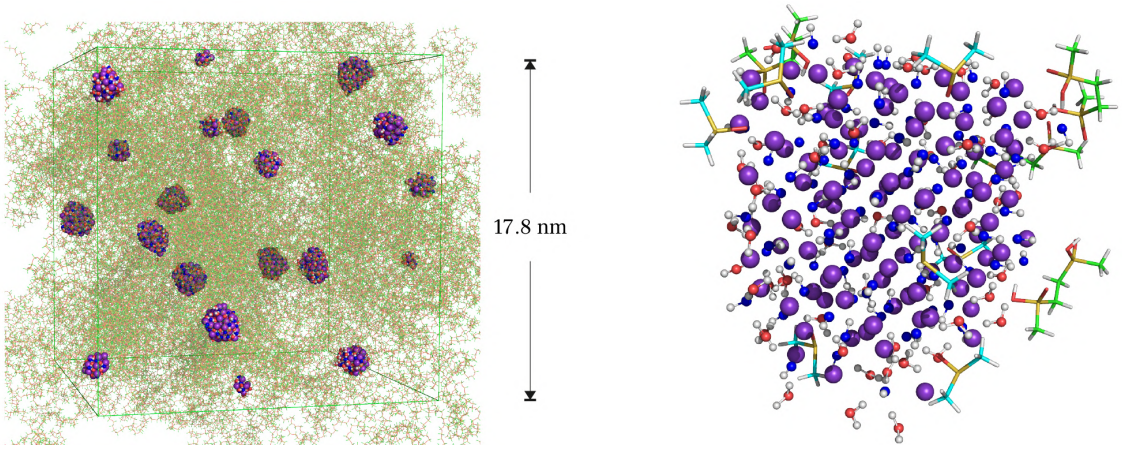

(c) Initiator effectiveness 13%

Figure 2. Condensed simulation cells with ionic aggragates (on the left) and organization of individual aggregates (on the right, the common color scheme is given on the top) at different effectivenes of KOH polymerization initiator

In the obtained MD simulations trajectories integrity of K^+ and OH^- aggregates and their coupling with water molecules or terminal PDMS residues were investigated. It was expected that the dynamics of inner layers (consisting of K^+ and OH^- ions) and outer layers (water, PDMS residues) of the aggregates could provide an insight into how the structure determines the materials properties, including the self-healing capacity.

As it was mentioned above, an increase in the amount of unreacted OH^- at reduced initiator effectiveness, enabled a formation of increasingly larger ionic clusters, where K^+ and OH^- alternate with each other. Thus, the considered decrease in initiator efficiency led to the formation of increasingly larger and rarified ionic aggregates in the bulk of polymeric cell. Additionally, significant differences in the dynamics of the aggregates were detected. During the simulation, the aggregates and their environment underwent two types of dynamic changes. The first one involved the aggregate "core" itself – the cluster of K^+ and OH^- ions – which could split into two parts with their subsequent separation (however, they could further merge again). These fission events were the more common, the higher the initiator efficiency was, i.e., the smaller were the clusters themselves. For the systems without any free OH^-, aggregates easily disintegrated, exchanged their core ions, or merged, as they were extremely small (with an average of 5 K^+ ions) and located close to each other (Tab. 1). As the ionic clusters grew with increasing of OH^- content, the aggregates became more stabilized. In particular, in systems with 10–13% efficiency, ion exchange between aggregates was practically non-existent; however, another interesting process prevailed.

The outer layer of such clusters, formed by water and chain end groups, proved to be even more mobile. Individual groups in this layer could reversibly separate from the cluster, and if the distance became large enough, return not to their own cluster, but to a neighbouring one. Thus, during the simulations, an exchange of outer layer components occurred between clusters. Expectedly, this exchange became more intense with increasing temperature. For PDMS-KOH-13 at room temperature, no such exchange events were observed within 0.5 μs of simulation, but as the temperature increased up to 100°C, the "hopping" of the PDMS termini between aggregates occurred many times within the same trajectory span (which is illustrated on Fig. 2). Since self-healing is always related with the redistribution of reversible interactions in the material, which provides the relative mobility of its chains, the redistribution of terminal PDMS groups between the aggregates in the MD trajectory might influence the self-healing mechanism of the PDMS-KOH material.

Water expectedly appeared to be the most mobile component of the outer layer of the aggregates, so the water exchange between aggregates was the most frequent event (see Tab. 1). It is to be established in further modeling, whether water exchange alleviates the inter-aggregate "hopping" of the PDMS residues and thus is an important active participant of the self-healing process, or this is an independent process.

With substitution of the KOH initiator with $N(CH_3)_4OH$ in the PDMS-TMAOH-13 systems, the behaviour of the aggregates was completely different. The aggregates themselves became unstable, when one part of them could shift and separate from another; however, such separations of the aggregates were reversible. What is more important, no exchange of PDMS residues between the outer aggregate layers was detected at either 25°C or 100°C. However, at all these temperatures, the real PDMS-TMAOH system provides self-healing. Therefore, the self-healing ability of PDMS-TMAOH systems should be mainly attributed to another physicochemical processes: general mobility of the PDMS chains coupled with ionic aggregates and "siloxane equilibration" reaction.

To the contrast, PDMS-KOH systems demonstrate a unique behaviour: rapid redistribution of internal noncovalent interactions between stable "anchor" aggregates. This process presumably can provide self-healing ability along with low viscosity, and thus could explain self-healing of PDMS-KOH with relatively good mechanical performance.

Conclusion

Molecular dynamic modelling of self-healing PDMS-based "siloxane equilibration" materials enabled to obtain the details of polydisperse structure depending on their composition. The main distinguishing feature of the systems with KOH or $N(CH_3)_4OH$ initiators was that initiator counterions are concentrated into aggregates, surrounded by negatively charged groups from the ends of the polymer chains. As initiator efficiency decreased, these aggregates became increasingly larger due to the intercalation of residual OH^- between potassium ions, additionally stabilizing these aggregates. They also coordinated the polar groups of the system around themselves: water molecules, as well as the initial polymer residues that carried the attached OH^- ion and the cross-linking residues. During the MD simulation of materials with KOH as initiator with 10–13% effectiveness at 100°C, these polar groups extensively migrated between stable ionic aggregates. Water was especially mobile in this regard, but the initial residues also underwent several "switches" during the 500 ns trajectory. At 25°C, these groups had insufficient kinetic energy to switch from one aggregate and attach to another one. These simulation data are in line with the experimental fact that the material with KOH as initiator undergoes self-healing only at the temperature above 100°C.

Another noteworthy point following from the MD results deserves special attention for the future study of self-healing properties. It is the balance between two interrelated processes: the "siloxane equilibration" reaction and the dynamic of ionic particles in self-healing process. If the reaction requires free $–(CH_3)_2SiO^-$ termini, which, according to the simulation data, are preferably bound with ionic aggregates, then the siloxane equilibration should be considered in the light of the aggregate structure. The aggregate itself, its size, compound and stability is expected to impact the kinetics of the "siloxane equilibration" reaction, and it is a comprehensive task for further investigations.

Thus, the structural models obtained via MD simulation condensation protocol discovered the existence of stable ionic aggregates in the PDMS polymer bulk. It enatails that the self-healing process can be determined by the structure and dynamics of these ionic aggregates, which would open new perspectives of modifications by controlling the size, distribution or kinetic parameters of group exchange of water-ionic aggregates in polydisperse multicomponent system.

Acknowledgements

This research was funded by the Ministry of Science and Higher Education of the Russian Federation (grant FENU 2024-0003).

The authors would like to express their acknowledgement to the Artificial Intelligence and Quantum Technologies (SEC "AIQ") Scientific and Educational Center of South Ural State University.

References

1. Bayly, C.I., Cieplak, P., Cornell, W.D., *et al.*: A well-behaved electrostatic potential based method using charge restraints for deriving atomic charges: The RESP model. Journal of Physical Chemistry 97(40), 10269–10280 (1993). https://doi.org/10.1021/j100142a004

2. Berendsen, H.J., Postma, J.P., Van Gunsteren, W.F., *et al.*: Molecular dynamics with coupling to an external bath. The Journal of Chemical Physics 81(8), 3684–3690 (1984). https://doi.org/10.1063/1.448118

3. Bergman, S.D., Wudl, F.: Re-Mendable Polymers. In: Self Healing Materials. Springer Series in Materials Science, pp. 45–68. Springer (2007). https://doi.org/10.1007/978-1-4020-6250-6_3

4. Bussi, G., Donadio, D., Parrinello, M.: Canonical sampling through velocity rescaling. Journal of Chemical Physics 126(1) (2007). https://doi.org/10.1063/1.2408420

5. Byrd, R.H., Lu, P., Nocedal, J., *et al.*: A Limited Memory Algorithm for Bound Constrained Optimization. SIAM Journal on Scientific Computing 16(5), 1190–1208 (1995). https://doi.org/10.1137/0916069

6. Chen, X., Dam, M.A., Ono, K., *et al.*: A thermally re-mendable cross-linked polymeric material. Science 295(5560), 1698–1702 (2002). https://doi.org/10.1126/science.1065879

7. Chen, Y., Tang, Z., Liu, Y., *et al.*: Mechanically Robust, Self-Healable, and Reprocessable Elastomers Enabled by Dynamic Dual Cross-Links. Macromolecules 52(10), 3805–3812 (2019). https://doi.org/10.1021/acs.macromol.9b00419

8. Cho, S.H., White, S.R., Braun, P.V.: Room-temperature polydimethylsiloxane-based self-healing polymers. Chemistry of Materials 24(21), 4209–4214 (2012). https://doi.org/10.1021/cm302501b

9. Cordier, P., Tournilhac, F., Soulié-Ziakovic, C., *et al.*: Self-healing and thermoreversible rubber from supramolecular assembly. Nature 451(7181), 977–980 (2008). https://doi.org/10.1038/nature06669

10. Cromwell, O.R., Chung, J., Guan, Z.: Malleable and Self-Healing Covalent Polymer Networks through Tunable Dynamic Boronic Ester Bonds. Journal of the American Chemical Society 137(20), 6492–6495 (2015). https://doi.org/10.1021/jacs.5b03551

11. Darden, T., York, D., Pedersen, L.: Particle mesh Ewald: An $N \cdot \log(N)$ method for Ewald sums in large systems. The Journal of Chemical Physics 98(12), 10089–10092 (1993). https://doi.org/10.1063/1.464397

12. Das, A., Sallat, A., Böhme, F., *et al.*: Ionic Modification Turns Commercial Rubber into a Self-Healing Material. ACS Applied Materials and Interfaces 7(37), 20623–20630 (2015). https://doi.org/10.1021/acsami.5b05041

13. Debsharma, T., Nguyen, L.T., Maliszewski, B.P., *et al.*: Eliminating creep in vitrimers using temperature-resilient siloxane exchange chemistry and N-heterocyclic carbenes. Chemical Science 16(21), 9337–9347 (2025). https://doi.org/10.1039/d4sc06278g

14. Deriabin, K.V., Filippova, S.S., Islamova, R.M.: Self-Healing Silicone Materials: Looking Back and Moving Forward. Biomimetics 8(3), 286 (2023). https://doi.org/10.3390/biomimetics8030286

15. Deriabin, K.V., Ignatova, N.A., Kirichenko, S.O., *et al.*: Structural features of polymer ligand environments dramatically affect the mechanical and room-temperature self-healing properties of cobalt(ii)-incorporating polysiloxanes. Organometallics 40(15), 2750–2760 (Jul 2021). https://doi.org/10.1021/acs.organomet.1c00392

16. Dong, X., Yuan, X., Song, Z., *et al.*: The development of an Amber-compatible organosilane force field for drug-like small molecules. Physical Chemistry Chemical Physics 23(22), 12582–12591 (2021). https://doi.org/10.1039/d1cp01169c

17. Du, G., Mao, A., Yu, J., *et al.*: Nacre-mimetic composite with intrinsic self-healing and shape-programming capability. Nature Communications 10(1) (2019). https://doi.org/10.1038/s41467-019-08643-x

18. Eisenberg, A., Hird, B., Moore, R.B.: A New Multiplet-Cluster Model for the Morphology of Random Ionomers. Macromolecules 23(18), 4098–4107 (1990). https://doi.org/10.1021/ma00220a012

19. Ghosh, K., Morgan, A., Garcia-Casas, X., *et al.*: Tailoring of Self-Healable Polydimethylsiloxane Films for Mechanical Energy Harvesting. ACS Applied Energy Materials 7(19), 8185–8195 (2024). https://doi.org/10.1021/acsaem.4c01275

20. He, C., Shi, S., Wang, D., *et al.*: Poly(oxime-ester) Vitrimers with Catalyst-Free Bond Exchange. Journal of the American Chemical Society 141(35), 13753–13757 (2019). https://doi.org/10.1021/jacs.9b06668

21. Hess, B., Bekker, H., Berendsen, H.J., *et al.*: LINCS: A Linear Constraint Solver for molecular simulations. Journal of Computational Chemistry 18(12), 1463–1472 (1997). https://doi.org/10.1002/(SICI)1096-987X(199709)18:12<1463::AID-JCC4>3.0.CO;2-H

22. Hess, B., Kutzner, C., Van Der Spoel, D., *et al.*: GRGMACS 4: Algorithms for highly efficient, load-balanced, and scalable molecular simulation. Journal of Chemical Theory and Computation 4(3), 435–447 (2008). https://doi.org/10.1021/ct700301q

23. Karatrantos, A.V., Couture, O., Hesse, C., *et al.*: Molecular Simulation of Covalent Adaptable Networks and Vitrimers: A Review. Polymers 16(10), 1373 (2024). https://doi.org/10.3390/polym16101373

24. Krug, D.J., Asuncion, M.Z., Laine, R.M.: Facile Approach to Recycling Highly Cross-Linked Thermoset Silicone Resins under Ambient Conditions. ACS Omega 4(2), 3782–3789 (2019). https://doi.org/10.1021/acsomega.8b02927

25. Lai, J.C., Jia, X.Y., Wang, D.P., *et al.*: Thermodynamically stable whilst kinetically labile coordination bonds lead to strong and tough self-healing polymers. Nature Communications 10, 1164 (2019). https://doi.org/10.1038/s41467-019-09130-z

26. Latif, S., Amin, S., Haroon, S.S., *et al.*: Self-healing materials for electronic applications: An overview. Materials Research Express 6(6) (2019). https://doi.org/10.1088/2053-1591/ab0f4c

27. Li, B., Cao, P.F., Saito, T., *et al.*: Intrinsically Self-Healing Polymers: From Mechanistic Insight to Current Challenges. Chemical Reviews 123(2) (2023). https://doi.org/10.1021/acs.chemrev.2c00575

28. Li, C.H., Wang, C., Keplinger, C., *et al.*: A highly stretchable autonomous self-healing elastomer. Nature Chemistry 8(6), 618–624 (2016). https://doi.org/10.1038/nchem.2492

29. Luo, F., Sun, T.L., Nakajima, T., *et al.*: Oppositely charged polyelectrolytes form tough, self-healing, and rebuildable hydrogels. Advanced Materials 27(17), 2722–2727 (2015). https://doi.org/10.1002/adma.201500140

30. Makarov, G.I., Makarova, T.M.: General AMBER force field parameters for modeling polyalkylsiloxane chains. Mendeleev Communications 35(2), 221–223 (2025). https://doi.org/10.71267/mencom.7580

31. Makarova, T.M., Bartashevich, E.V.: Construction of Self-Healing PDMS Materials Models by Supercomputer MD Simulations. In: 19th Proceedings of the International Scientific Conference, PCT'2025, Moscow, Russia, April 8-10, 2025, pp. 36–43. Chelyabinsk: Publishing of the South Ural State University (2025). https://doi.org/10.14529/pct2025

32. Mark, J.E.: Some interesting things about polysiloxanes. Accounts of Chemical Research 37(12), 946–953 (2004). https://doi.org/10.1021/ar030279z

33. Miranda, I., Souza, A., Sousa, P., *et al.*: Properties and applications of PDMS for biomedical engineering: A review. J. Funct. Biomater. 13(1), 2 (2022). https://doi.org/10.3390/jfb13010002

34. Oh, J.Y., Son, D., Katsumata, T., *et al.*: Stretchable self-healable semiconducting polymer film for active-matrix strain-sensing array. Science Advances 5(11) (2019). https://doi.org/10.1126/sciadv.aav3097

35. Oku, T., Furusho, Y., Takata, T.: A concept for recyclable cross-linked polymers: Topologically networked polyrotaxane capable of undergoing reversible assembly and disassembly. Angewandte Chemie - International Edition 43(8), 966–969 (2004). https://doi.org/10.1002/anie.200353046

36. Osthoff, R.C., Bueche, A.M., Grubb, W.T.: Chemical Stress-Relaxation of Polydimethylsiloxane Elastomers. Journal of the American Chemical Society 76(18), 4659–4663 (1954). https://doi.org/10.1021/ja01647a052

37. Peng, Y., Zhao, L., Yang, C., *et al.*: Super tough and strong self-healing elastomers based on polyampholytes. Journal of Materials Chemistry A 6(39), 19066–19074 (2018). https://doi.org/10.1039/c8ta06561f

38. Prokudin, A.V., Dziuba, M.A., Safonov, V.I., *et al.*: Self-healing "siloxane equilibrium" materials after low-power electric breakdown in small-volume cells. Mendeleev Commun. 36(3), 308–310 (2026). https://doi.org/10.71267/mencom.7926

39. Raj M, K., Chakraborty, S.: PDMS microfluidics: A mini review. Journal of Applied Polymer Science 137(27), 48958 (2020). https://doi.org/10.1002/app.48958

40. Rao, Y.L., Chortos, A., Pfattner, R., *et al.*: Stretchable self-healing polymeric dielectrics cross-linked through metal-ligand coordination. Journal of the American Chemical Society 138(18), 6020–6027 (2016). https://doi.org/10.1021/jacs.6b02428

41. Rashevskii, A.A., Deriabin, K.V., Parshina, E.K., *et al.*: Self-healing redox-active coatings based on ferrocenyl-containing polysiloxanes. Coatings 13(7), 1282 (Jul 2023). https://doi.org/10.3390/coatings13071282

42. Rekondo, A., Martin, R., Ruiz De Luzuriaga, A., *et al.*: Catalyst-free room-temperature self-healing elastomers based on aromatic disulfide metathesis. Materials Horizons 1(2), 237–240 (2014). https://doi.org/10.1039/c3mh00061c

43. Rutenbar, R.A.: Simulated annealing algorithms: An overview. IEEE Circuits and Devices Magazine 5(1), 19–26 (1989). https://doi.org/10.1109/101.17235

44. Saed, M.O., Terentjev, E.M.: Siloxane crosslinks with dynamic bond exchange enable shape programming in liquid-crystalline elastomers. Scientific Reports 10(1), 6609 (2020). https://doi.org/10.1038/s41598-020-63508-4

45. Seethapathy, S., Górecki, T.: Applications of polydimethylsiloxane in analytical chemistry: A review. Analytica Chimica Acta 750, 48–62 (2012). https://doi.org/10.1016/j.aca.2012.05.004

46. Sharma, H., Rana, S., Singh, P., *et al.*: Self-healable fiber-reinforced vitrimer composites: overview and future prospects. RSC Adv. 12(50), 32569–32582 (2022). https://doi.org/10.1039/d2ra05103f

47. Taynton, P., Yu, K., Shoemaker, R.K., *et al.*: Heat- or water-driven malleability in a highly recyclable covalent network polymer. Advanced Materials 26(23), 3938–3942 (2014). https://doi.org/10.1002/adma.201400317

48. Van Der Spoel, D., Lindahl, E., Hess, B., *et al.*: GROMACS: Fast, flexible, and free. J. Comput. Chem. 26, 1701–1718 (2005). https://doi.org/10.1002/jcc.20291

49. Wang, J., Wolf, R.M., Caldwell, J.W., *et al.*: Development and testing of a general Amber force field. Journal of Computational Chemistry 25(9), 1157–1174 (2004). https://doi.org/10.1002/jcc.20035

50. Wang, P., Wang, Z., Liu, L., *et al.*: Self-Healable and Reprocessable Silicon Elastomers Based on Imine–Boroxine Bonds for Flexible Strain Sensor. Molecules 28(16), 6049 (2023). https://doi.org/10.3390/molecules28166049

51. Weng, G., Thanneeru, S., He, J.: Dynamic Coordination of Eu–Iminodiacetate to Control Fluorochromic Response of Polymer Hydrogels to Multistimuli. Advanced Materials 30(11), 1706526 (2018). https://doi.org/10.1002/adma.201706526

52. Wu, J., Cai, L.H., Weitz, D.A.: Tough Self-Healing Elastomers by Molecular Enforced Integration of Covalent and Reversible Networks. Advanced Materials 29(38), 1702616 (2017). https://doi.org/10.1002/adma.201702616

53. Yang, X., Huang, W., Dong, H., *et al.*: Smart Polydimethylsiloxane Materials: Versatility for Electrical and Electronic Devices Applications. Advanced Materials 37(17), 2500472 (2025). https://doi.org/10.1002/adma.202500472

54. Yao, Y., Tai, H., Wang, D., *et al.*: One-pot preparation and applications of self-healing, self-adhesive PAA-PDMS elastomers. Journal of Semiconductors 40(11) (2019). https://doi.org/10.1088/1674-4926/40/11/112602

55. Ye, G., Wang, C., Guo, Y., *et al.*: Vitrimer as a Sustainable Alternative to Traditional Thermoset: Recent Progress and Future Prospective. ACS Polymers Au 5(5), 445–457 (2025). https://doi.org/10.1021/acspolymersau.5c00081

56. Ying, H., Zhang, Y., Cheng, J.: Dynamic urea bond for the design of reversible and self-healing polymers. Nature Communications 5 (2014). https://doi.org/10.1038/ncomms4218

57. Yoshida, S., Ejima, H., Yoshie, N.: Tough Elastomers with Superior Self-Recoverability Induced by Bioinspired Multiphase Design. Advanced Functional Materials 27(30) (2017). https://doi.org/10.1002/adfm.201701670

58. Zhang, K., Sun, J., Song, J., *et al.*: Self-Healing Ti3C2MXene/PDMS Supramolecular Elastomers Based on Small Biomolecules Modification for Wearable Sensors. ACS Applied Materials and Interfaces 12(40), 45306–45314 (2020). https://doi.org/10.1021/acsami.0c13653

59. Zheng, P., McCarthy, T.J.: A surprise from 1954: Siloxane equilibration is a simple, robust, and obvious polymer self-healing mechanism. Journal of the American Chemical Society 134(4), 2024–2027 (2012). https://doi.org/10.1021/ja2113257

60. Zou, Z., Zhu, C., Li, Y., *et al.*: Rehealable, fully recyclable, and malleable electronic skin enabled by dynamic covalent thermoset nanocomposite. Science Advances 4(2) (2018). https://doi.org/10.1126/sciadv.aaq0508